An effective formulation for estimating wetland surface energy fluxes from weather data

Yi Wang[1], Richard. M. Petrone[1]

[1]Hydrometeorology Research Group, University of Waterloo, Waterloo, Ontario, Canada, N2L 3G1

Abstract: In modelling evapotranspiration, the need for land surface variables including ground heat fluxes (G), surface temperature (T_s), surface relative humidity (RH_s) and surface resistance often present a challenge due to land heterogeneity and limited measurements. This study introduces a simple formulation rooted in the shared physical basis of the maximum entropy model (MaxEnt), the Relative Humidity at Equilibrium (ETRHEQ) method, and the Surface Flux Equilibrium (SFE) method, and it estimates sensible (H) and latent fluxes (LE) in wetlands without requiring land surface variables or site-specific calibration, except for an assumed vegetation height. Further, it effectively estimates LE from half-hourly to monthly scales in FLUXNET and AmeriFlux wetland sites. While its performance in estimating H is less satisfactory due to loosely constrained boundary conditions, it shows promising potential for simultaneously and precisely estimating LE, H, G, T_s, and RH_s from weather data in various ecosystems.

Key points:

1. The formulation is based on the principle of maximum Shannon information entropy production for turbulence fluxes.

2. The formulation does not require land surface variables or site-specific calibration; only an assumed vegetation height is needed.

3. The formulation effectively estimates LE from half-hourly to monthly scales.

Plain language summary: This study introduces a new method to predict how much water and heat wetlands transport to the atmosphere, a process that is usually complicated because it involves a lot of detailed information about land properties that are hard to measure. This new method does not need all those details, and instead just needs an estimate of how tall the plant canopy is. This method works extremely well for predicting water release into the air over periods ranging from half-hourly to monthly in FLUXNET and AmeriFlux wetland sites. Although this method is not perfect at predicting heat release due to some assumptions that have to be made about ground heat and surface temperature, it shows a lot of promise. With a bit of fine-tuning, it could be used to accurately measure both water and heat exchanges in various types of ecosystems, not just wetlands.

1. Introduction

The partitioning of energy on the land surface of terrestrial ecosystems into ground heat (G), sensible heat (H) and latent heat (LE) has long been recognized as a result of complex interactions between atmospheric and land surface properties (Duveiller et al., 2018; Forzieri et al., 2020; Williams and Torn, 2015; Wilson et al., 2002). At short temporal scales, it is impacted by plant physiological activities and boundary layer properties, and over the long term, the biogeochemical cycling, disturbance, and climate all have significant roles to play (Arneth et al., 2012; Green et al., 2017; Wilson et al., 2002). While the importance of land surface properties

cannot be overlooked, land surface variables are a challenge to parameterize due to land heterogeneity and varied physiological responses of vegetation to changing environmental conditions (Dickinson et al., 1991; Mueller and Seneviratne, 2014; Wang and Dickinson, 2012).

Recent studies proposed two methodologies, namely the Relative Humidity at Equilibrium (ETRHEQ) method and the Surface Flux Equilibrium (SFE) method, to estimate surface energy fluxes from near-surface atmospheric conditions (McColl et al., 2019; Salvucci and Gentine, 2013). ETRHEQ determines the optimal daily surface conductance that yields the most accurate ET predictions based on minimum vertical variance of relative humidity (RH) (Salvucci and Gentine, 2013), and SFE provides the solution of ETRHEQ at the steady state (McColl et al., 2019). The two methods are justified by strong land-atmospheric coupling wherein land surface properties are embedded in the near-surface atmospheric conditions (McColl and Rigden, 2020; McColl et al., 2019). Conversely, the conditions of the near-surface atmosphere are also reflected in land surface variables, which partly justifies another methodology called the maximum entropy model (MaxEnt) that estimates surface energy fluxes using only the surface temperature and surface relative humidity in addition to net radiation (Wang and Bras, 2011; Wang and Bras, 2009). Although the three models have shown success over a variety of ecosystems worldwide (Chen et al., 2021; McColl and Rigden, 2020; Rigden and Salvucci, 2015; Yang et al., 2022), each have their own limitations. ETRHEQ requires vegetation height and ground heat fluxes in addition to 24-hour subdaily weather measurements, to estimate latent and sensible fluxes at the daily scale (Rigden and Salvucci, 2015; Salvucci and Gentine, 2013). SFE, though it requires less parameters (i.e., only net radiation, ground heat flux, air temperature and air specific humidity), works for sites near or at the steady state and estimates energy fluxes at the daily or larger temporal scales (Chen et al., 2021; Kim et al., 2023; McColl and Rigden, 2020). The

MaxEnt model is formulated based on minimizing the dissipation function of turbulent fluxes (which is equivalent to maximizing Shannon information entropy production of the turbulent fluxes (Dewar, 2005)) and the Monin-Obukhov similarity theory (MOST)'s extremum solution (Wang and Bras, 2009), but the justification of extremum solution still requires further examination (Wang and Bras, 2010; Wang et al., 2023).

Wang et al. (2023) investigated the linkage of the three models and found that minimizing the dissipation function of energy fluxes in MaxEnt is equivalent to minimizing the vertical variance of RH in ETRHEQ. The empirical success of the three models is explained by the fact that far-from-equilibrium ecosystems progress toward a steady state (i.e., the SFE state) by minimizing dissipation, and this tendency is manifested through the vertical variance of RH (Wang et al., 2023). In addition, Wang et al. (2023) demonstrated that the connection among the three models is independent of Monin-Obukhov similarity theory (MOST)'s extremum solution (Wang et al., 2023), and proposed a more general formulation describing the dissipation function (D) of energy fluxes for both non-steady and steady states, as:

$$D = \frac{2G^2}{I_s} + \frac{2H^2}{I_a} + \frac{LE^2}{I_e} \quad (1)$$

$$\text{with } I_s = \sqrt{I_d^2 + \theta\, I_w^2},\ I_a = \rho c_p \sqrt{g_a},\ \text{and } I_e = \frac{\delta}{\gamma} R H_s I_a.$$

where I_s, I_a and I_e are the thermal inertia parameters for G, H and LE, respectively; The parameterization of I_s is provided in Huang et al. (2017) and Yang et al. (2022) in which I_d is the thermal inertia of dry soil; θ is the volumetric soil moisture; I_w is the thermal inertia of still liquid water; ρ is the density of air; c_p is the specific heat capacity of air; g_a is the aerodynamic conductance; δ is the slope of the relation between saturated specific humidity and temperature,

89 $\gamma = \frac{c_p}{\lambda}$ with λ being the latent heat of vaporization of water; and RH_s is the surface relative
90 humidity. The detailed formulation will be introduced in the next section.

91 The new formulation is denoted as MaxEnt-ETRHEQ, indicating the shared physical basis
92 underlying MaxEnt and ETRHEQ. It appears to require both atmospheric and land surface
93 variables at first glance. However, closer scrutiny revealed that land surface variables such as
94 surface temperature, surface relative humidity and soil moisture are interlinked in the calculation
95 of G, H and LE under energy closure. This interconnection renders the formulation self-
96 constrained. Consequently, the energy fluxes and the land surface variables can be analytically
97 determined by identifying the minimum value of D given suitable ranges of surface temperature
98 and relative humidity. Therefore, MaxEnt-ETRHEQ has potential to estimate surface energy
99 fluxes for various ecosystems, with minimal or no land surface information. But its effectiveness
100 is yet to be examined. Leveraging our proficiency and background in wetland ecosystems, we
101 demonstrate in this paper that MaxEnt-ETRHEQ is an effective formulation for estimating
102 energy fluxes for wetland ecosystems, especially for estimating LE from subdaily to monthly
103 scales, and it does not necessities any land surface parameters; only an assumption regarding
104 vegetation height is required.

105

106 **2. Methods**

107 2.1 The formulation of MaxEnt-ETRHEQ

108 The main formula of MaxEnt-ETRHEQ is given as Eq. 1. The required input parameters are
109 atmospheric pressure (p), air temperature (T_a), wind speed (u), friction velocity (u*), air relative
110 humidity (RH), net radiation (R_n), the height of the measurements of weather data (z) and

vegetation height (z_{veg}). Meanwhile, MaxEnt-ETRHEQ will automatically create two variables, surface temperature (T_s) and surface relative humidity (RH_s) within a pre-defined range for studied ecosystems (will be explained later).

The surface pressure (p_s) is calculated from the atmospheric pressure by rearranging the formulas used in ETRHEQ, as (Salvucci and Gentine, 2013):

$$p_s = \frac{p}{\exp(\frac{-gz}{R_d T_a})} \quad (2)$$

where p_s is the surface pressure (Pa), p is the atmospheric pressure (Pa), g is the gravitational constant (9.8 $m \cdot s^{-2}$), z is the height of the measurements of weather data (m), Rd is the gas constant for dry air (287 $J \cdot kg^{-1} \cdot K^{-1}$), and T_a is the air temperature (K). Saturation vapor pressure (e*) is calculated from integrated Clausius–Clapeyron relation, as (Salvucci and Gentine, 2013):

$$e^*(T_a) = 611.2 \times \exp(\frac{17.67 \times (T_a - 273.15)}{T_a - 29.65}) \quad (3)$$

$$e^*(T_s) = 611.2 \times \exp(\frac{17.67 \times (T_s - 273.15)}{T_s - 29.65}) \quad (4)$$

where $e^*(T_a)$ and $e^*(T_s)$ are saturation vapor pressure (Pa) at air temperature (T_a, K) and surface temperature (T_s, K), respectively.

Saturated specific humidity (q*) is related to the saturation vapor pressure (e*) through the following equations (Salvucci and Gentine, 2013):

$$q^*(T_a) = \frac{\epsilon e^*(T_a)}{p - (1-\epsilon) e^*(T_a)} \quad (5)$$

$$q^*(T_s) = \frac{\epsilon e^*(T_s)}{p_s - (1-\epsilon) e^*(T_s)} \quad (6)$$

where ϵ is the dimensionless ratio of the gas constant for dry air to water vapor (0.622).

Using Eq. 5 and 6, the slope of the relation between saturated specific humidity (q*) and temperature (T) can be linearly extrapolated following (Kim et al., 2021; McColl et al., 2019):

$$\delta = \frac{q^*(T_s) - q^*(T_a)}{T_s - T_a} \quad (7)$$

where $q^*(T_s)$ and $q^*(T_a)$ are the surface and atmospheric saturated specific humidity ($kg \cdot kg^{-1}$), respectively, and T_s and T_a are the surface and air temperature (K), respectively.

The sensible and latent heat fluxes are calculated using the flux gradient equations, as (Kim et al., 2021):

$$H = \rho c_p g_a (T_s - T_a) \quad (8)$$

$$LE = \lambda \rho g_a (q_s - q_a) \quad (9)$$

where H and LE are the sensible and latent heats ($W \cdot m^{-2}$), ρ is the density of air ($\rho = \frac{p}{R_d T_a}$, $kg \cdot m^3$), c_p is the specific heat of air at constant pressure (1004.7 $J \cdot kg^{-1} \cdot °C^{-1}$), g_a is the aerodynamic conductance accounting for atmospheric stability ($m \cdot s^{-1}$), λ is the latent heat of vaporization (2.502×10^6 $J \cdot kg^{-1}$), q_s is the surface specific humidity ($q_s = RH_s \cdot q^*(T_s)$, $kg \cdot kg^{-1}$), and q_a is the air specific humidity ($q_a = RH \cdot q^*(T_a)$, $kg \cdot kg^{-1}$).

The aerodynamic conductance under the neutral atmospheric condition (g_{a_n}) is given by Allen et al. (1998), as:

$$g_{a\_n} = \frac{\kappa^2 u}{\ln\left(\frac{z-d}{z_{om}}\right) \ln\left(\frac{z-d}{z_{oh}}\right)} \quad (10)$$

with κ being the von Karman constant (0.41), u being the wind speed ($m \cdot s^{-2}$), z being the height of height of the measurements of wind speed (m), d being the zero-plane displacement height

(m), z_{om} is the roughness length governing momentum transfer (m), and z_{oh} is the roughness length governing transfer of heat and vapour (m)

When no vegetation is present in the study sites (z_{veg} =0 m), d is set as 0 m, with both z_{om} and z_{oh} being set as 0.001 m; whereas in the presence of vegetation, d is set as 0.7 of z_{veg}, with z_{om} being 0.1 of z_{veg}, and z_{oh} being estimated using kB^{-1} approach, following Salvucci and Gentine (2013):

$$\kappa B^{-1} = \ln(\frac{z_{om}}{z_{oh}}) \cong \kappa(6Re^{\frac{1}{4}} - 5) \quad (11)$$

where Re is the roughness Reynolds number ($Re = \frac{u^* z_{om}}{\nu}$, with u* is the friction velocity ($m \cdot s^{-2}$) and ν being the kinematic viscosity, as 1.45×10^{-5} $m^2 \cdot s^{-1}$).

To account for atmospheric stability, the actual aerodynamic conductance (g_a, $m \cdot s^{-1}$) is calculated following Merlin et al. (2016), as:

$$g_a = (1 + R_i)^{\eta} \cdot g_{a\_n} \quad (12)$$

$$R_i = \frac{\beta_{thermal} \times gz(T_s - T_a)}{T_a u^2} \quad (13)$$

where $\beta_{thermal}$ is the thermal expansion coefficient, and $\beta_{thermal}$ =5 was used following Choudhury et al. (1986) and Merlin et al. (2011); g is the gravitational constant (9.8 $m \cdot s^{-2}$), T_s is the surface soil temperature (K), T_a is the air temperature (K). In Eq. (11), the coefficient η is set to 0.75 in unstable conditions ($T_s > T_a$) and to 2 in stable conditions ($T_s < T_a$); u is the wind speed ($m \cdot s^{-1}$) and z is the height (m) at which wind speed was measured.

The ground heat flux (G, $W \cdot m^{-2}$) is calculated using energy balance equation as:

$$G = R_n - H - LE \quad (14)$$

where Rn is the net radiation ($W \cdot m^{-2}$), and H and LE are calculated based on Eq. 8 and 9.

The parameterization of thermal inertias (I_s, I_a and I_e) is provided in Eq. 1. To minimize the land surface parameters needed in the MaxEnt-ETRHEQ formulation, I_s is set as a constant (1300 $J \cdot m^{-2} \cdot K^{-1} \cdot s^{-1/2}$, i.e., tiu) following Rigden and Salvucci (2017). It is postulated that such a constant is acceptable, because: (1) Rigden and Salvucci (2015) stated that the optimal range of I_s was between 300 and 1000 tiu for AmeriFlux sites, and as I_s increases with wetter soils, it should be slightly higher than the optimal range; (2) Rigden and Salvucci (2017) used the calibrated I_s of 1300 tiu for their study sites across united states; (3) the modelling results agree well with the eddy covariance measurements (presented in the results section); and (4) using measured soil moisture did not significantly improve the modelling performance (presented in Table S4).

The last step is to specify appropriate ranges of G, T_s and RH_s. Without this specification, G could become unrealistically large, which does not occur in the real world. After specifying the ranges, the dissipation function D is computed for every set of input weather data and every possible paring of G, T_s and RH_s. The selection of the optimal set of G, T_s and RH_s will be done through finding the minimum D. Once these optimal values are found, H and LE are concurrently determined through the calculations from Eq.1 to 14.

2.2 The boundary conditions for wetland ecosystems

The upper limit of G for wetland ecosystems is set as 0.20 of Rn based on the empirical relationship between G and Rn used in GLEAM model: G/Rn = 0.20 for short vegetation (0.05 m < z_{veg} <1 m) and G/Rn = 0.15 for tall vegetation (Z_{veg} >1 m) (Miralles et al., 2011). T_s and T_a at the 2 m height above land surface may differ by several °C, but the difference between maximum T_a and maximum T_s may vary up to 30 °C (Good et al., 2017; Mildrexler et al., 2011),

so T_s is set to $T_a \pm 30$ °C. Typically, RH_s must be higher than RH for evapotranspiration to occur. As evapotranspiration progresses, RH tends to increase while RHs decreases until the ecosystem reaches the surface flux equilibrium state (RH_{eq}=RH=RH_s). This suggests that there exists a boundary for RH_s, which falls within the range of RH and RH_{eq}. To estimate RH_{eq}, the Priestley-Taylor equation for water body (i.e., the left of the equals sign of Eq. 15) (Priestley and Taylor, 1972) is combined with the PM_{RH} equation under RH=RH_s (the right of the equals sign of Eq. 15) (Kim et al., 2021) to determine the maximum RH_{eq}, as:

$$1.26\lambda(R_n - G)\frac{\Delta}{\Delta+\gamma'} = \frac{RH_{eq}\Delta}{RH_{eq}\Delta+\gamma'}(R_n - G) \quad (15)$$

where 1.26 is the Priestley-Taylor coefficient for open water; λ is the latent heat of vaporization (2.502×10^6 J·kg^{-1}); Rn is the net radiation (W·m^{-2}); G is the ground heat flux (W·m^{-2}); Δ is the slope of the relation between saturation vapor pressure and temperature (Pa·°C^{-1}); γ' is the psychrometric constant ($\gamma' = \frac{pc_p}{\epsilon\lambda}$, with being is the air pressure (Pa), c_p being the specific heat of air at constant pressure (1004.7 J·kg^{-1}·°C^{-1}), ϵ being the dimensionless ratio of the gas constant for dry air to water vapor (0.622), and); and λ being the latent heat of vaporization (2.502×10^6 J·kg^{-1})); and RH_{eq} is the equilibrium RH of a saturated wetland ecosystem. Rearranging Eq. 15 leads to the expression of RH_{eq}, as:

$$RH_{eq} = \frac{1.26\lambda\gamma'}{\Delta(1-1.26\lambda)+\gamma'} \quad (16)$$

There are multiple ways to estimate Δ. In this study, the method provided in the FAO Penmen-Monteith equation is chosen to estimate Δ from T_a, as (Allen et al., 1998):

$$\Delta = \frac{1000 \times 4098[0.6108\exp(\frac{17.27(T_a - 273.15)}{(T_a - 273.15)+237.3}]}{(T_a - 273.15 + 237.3)^2} \quad (17)$$

where 1000 is a unit conversion coefficient, T_a is the air temperature (K).

It is important to recognize that the range for G, T_s and RH_s can be refined in various ways. The ranges defined above are just simple examples to determine the plausible ranges of these parameters in wetland ecosystems, achieving more realistic results while reducing computation time. The true ranges for G, T_s, and RH_s might be more constrained than these estimated values. And many models, especially the models of G (e.g., the models listed in Purdy et al. (2016), can be coupled with MaxEnt-ETRHEQ formulation. Exploring the potential enhancement of MaxEnt-ETRHEQ's performance by integrating these models presents an intriguing subject for future research.

3. Data and model evaluation

3.1 Data

All wetland sites classified as WET under the Vegetation IGBP category from the FLUXNET 2015 (Pastorello et al., 2020) and AmeriFlux (ameriflux.lbl.gov) FULLSET data products, shared under the CC-BY-4.0 license, were chosen for this study. The characteristics of the sites include latitude, longitude, elevation, mean measurement height, mean vegetation height, mean annual temperature, mean annual precipitation, and the distance to the coast (Table S1 and Table S2). Sites within 25 miles (~40 km) of the coast were removed, as ETRHEQ does not perform well in coastal regions (Rigden and Salvucci, 2015). In addition, the sites without the measurements of Rn and G were removed. The filter process results in 11 sites, including CZ-wet (Dušek et al., 2016), DE-SfN (Klatt et al., 2016), DE-Zrk (Sachs et al., 2016), FI-Lom (Aurela et al., 2016),

US-Atq (Zona and Oechel, 2016a), US-BZB (Euskirchen, 2021a), US-BZF (Euskirchen, 2021b), US-BZo (Euskirchen, 2022), US-ICs (Euskirchen et al., 2016), US-Ivo (Zona and Oechel, 2016b), and US-Los (Desai, 2016).

For every site, its fullset product encompasses five separate datasheets, containing measurements of atmospheric variables and energy fluxes at half-hourly, daily, weekly, monthly, and annual scales. At each temporal scale, u*("USTAR"), RH ("RH"), and Rn ("NETRAD") as well as gap-filled atmospheric measurements (denoted with the "_F" qualifier), including p ('PA_F"), T_a ("TA_F"), u ("WS_F"), and VPD ("VPD_F"), and the energy fluxes with marginal distribution sampling gap-filling method, which are G ("G_F_MDS"), H ("H_F"MDS"), and LE ("LE_F_MDS") were obtained. The names enclosed in double quotes within brackets in the above sentence represent the variable names in the data products. RH at daily or larger scales was not directly available, so it was estimated from VPD and T_a using the Clausius–Clapeyron relation. Besides z and z_{veg} were provided in Table S1 and S2. For sites where z_{veg} is not available, a value of 0.5 to z_{veg} was assigned.

The focus here was limited to temporal scales between half-hourly and monthly, due to a lack of adequate sites and measurements for conducting a robust analysis at the yearly level. At the half-hourly scale, data with poor quality (i.e., the quality flag (QC) >1) were removed. At coarser temporal resolutions, i.e., from daily to monthly, only the measured data (QC=0) or the gap-filled data where over 80% measured or good quality gap-filled (QC=1) records aggregated from finer temporal resolutions were included, consistent with Kim et al. (2023). As a result, FI-Lom were removed from daily to monthly scales due to the lack of the quality flag for G. At the monthly scale, DE-sfN was also removed because only one measurement was available. In addition, measurements were also removed if the surface energy imbalance was greater than 50 $W \cdot m^{-2}$

(McColl and Rigden, 2020; Rigden and Salvucci, 2015) or Rn - G was negative (Kim et al., 2023). The amount of data after all filters from half-hourly to monthly scales are presented in Table S3. The model was also run for sites where soil moisture measurements were available (i.e., US-BZB, US-BZF, US-BZo and US-ICs), to assess whether incorporating soil moisture would enhance the model's performance, and the error statistics are provided in Table S4.

3.2 Model evaluation

The root-mean-square error (RMSE), slope and intercept (i.e., bias) of the fitted linear relationship between modelled and measured energy fluxes, and the coefficient of determination (R^2) were used as metrics to evaluate model performance. The evaluation was made of the measurements without energy closure correction (specifically, “H_F_MDS” and “LE_F_MDS” in the data product) and with correction using the energy balance closure correction factor on the assumption that the Bowen ratio is correct (Pastorello et al., 2020) (the corrected energy fluxes are “H_CORR” and “LE_CORR” in the data product), respectively. In addition, H_F_MDS and LE_F_MDS were compared with H and LE calculated as the residual of the energy balance (i.e., H_re = Rn - G_F_MDS - LE_F_MDS, and LE_re = Rn - G_F_MDS - H_F_MDS) to assess the how energy imbalance and the inherent uncertainty in the eddy covariance measurements affect the evaluation of the performance of the model. If there is no energy closure problems in the eddy covariance measurements, there would be a perfect fit between the measurements and the residuals of the energy balance for each energy flux. This represents the highest level of performance that can be expected from any model in comparison to eddy covariance measurements, as explained in McColl and Rigden (2020). However, comparisons with other models such as Penman-Monteith, Priestley-Taylor, MaxEnt, ETRHEQ, SFE, or MEP-SFE were not conducted because MaxEnt-ETRHEQ is still in its early stage, and this paper is intended to

provide a possible way to utilize it for wetland ecosystems. Further, MaxEnt-ETRHEQ is unique as it does not require G or T_s as inputs, unlike other models. However, inter-model comparisons will be considered in future research.

All the analysis was conducted on R 4.3.0 (R Core Team 2023). The R scripts, which contain the codes for calculating the distance from study sites to the coast, modelling the energy fluxes using MaxEnt-ETRHEQ for each site, and creating the figures presented in this paper, are all available at Wang (2024).

4. Results

MaxEnt-ETREHQ provides highly accurate predictions for LE from half-hourly to monthly scales (Figure 1), with slopes ranging from 0.86 to 1.08 and biases ranging from 4.00 to 6.34 $W \cdot m^{-2}$. When the energy balance residuals (e.g., H_re and LE_re) were used to compare with the measurements (H_F_MDS and LE_F_MDS), their values of R^2 and the proximity of the slopes to 1 show similar levels with MaxEnt-ETRHEQ, but their bias, which is around 14 to16 $W \cdot m^{-2}$ and RMSE, which around 23 to 28 $W \cdot m^{-2}$ (Table 1), were slightly larger than those of MaxEnt-ETRHEQ (bias: 4 to 7 $W \cdot m^{-2}$ and RMSE:11 to 27 $W \cdot m^{-2}$). In this sense, the error statics of MaxEnt-ETRHEQ for estimating LE are slightly better than the errors statistics from the eddy covariance measurements (Table 1).

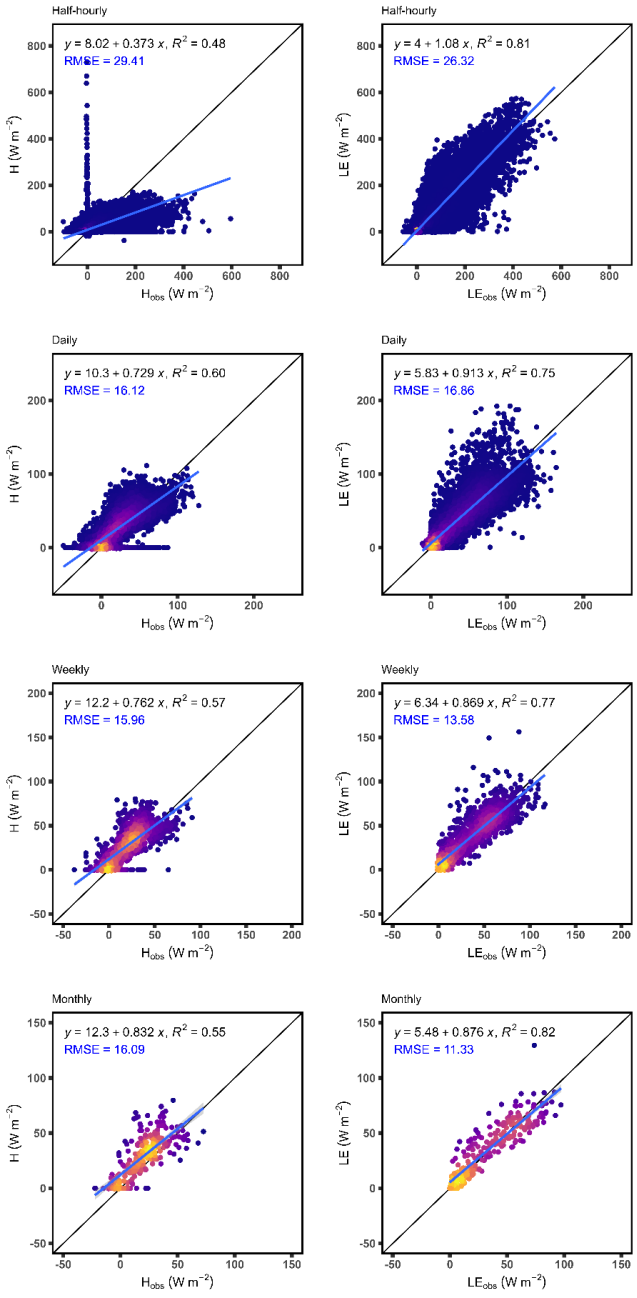

297

298 **Figure 1. Modelled H and LE versus measurements (H_{obs} and LE_{obs}) without energy**
299 **balance closure correction from half-hourly to monthly scales. The blue lines represent the**
300 **fitted linear regressions. The black lines are 1:1 lines. The color of the points represents the**
301 **density of the data ranging from low (purple) to medium (red) to high (yellow).**

302

303 On the other hand, the model does not predict H with the same performance as it predicts LE,

304 especially at the half-hourly scale (Figure 1). But when the time scale becomes larger, the

performance on estimating H is improved (Figure 1 and Table 1). Overall, MaxEnt-ETRHEQ tends to overestimate H when H is low and underestimate H when it is high (Figure 1). Given the estimation of LE was quite accurate, the less satisfactory performance of MaxEnt-ETRHEQ for H can be attributed to less accurately defined boundary conditions for G and T_s. In the current model setting, G was limited to up to 20% percent of Rn based on the GLEAM model that was designed for daily applications (Purdy et al., 2016). This explains why MaxEnt-ETRHEQ performs better in estimating H at daily and larger time scales. But at most study sites, G often exceeds 20% of Rn when Rn is exceptionally low (e.g., less than 50 $W \cdot m^{-2}$), and frequently falls below 10% of Rn when Rn is high (greater than 400 $W \cdot m^{-2}$). Therefore, when Rn is low, G is underestimated, leading to an overestimation of H, and vice versa.

At the half-hourly scale, there is a spike of estimated H when measured H is near zero (Figure 1). The spike is only from the US-BZo site (Figure S1) that happened during the night when Rn, G_F_MDS, H_F_MDS and LE_F_MDS were all negative, and the absolute value of G was at least 10 times larger than that of Rn. These energy fluxes suggest that US-BZo likely encountered intense convective weather at these periods, characterized by air that was warmer and more humid than the surface, accompanied by significant condensation. Under these weather circumstances, the current MaxEnt-ETRHEQ formulations were unsuitable for H, LE, and g_a. Determining the applicability of Eq. 1 in such conditions and devising revisions for the calculations of H, LE, and g_a need to be addressed in future research.

When H and LE observations are adjusted to force energy balance closure (i.e., H_CORR and LE_CORR), the performance of MaxEnt-ETRHEQ did not seem improve overall. For example, the bias in H or LE estimations decrease when the energy fluxes are corrected at all temporal scales, but the R^2, RMSE and slopes deteriorate (Table 1). This is because the energy balance

closure correction results in higher H and LE for most of the study sites. While this adjustment could result in more accurate energy fluxes, it also has the potential for overcorrection as diagnosed in Mauder et al. (2018). Consequently, the actual performance of MaxEnt-ETRHEQ in estimating H and LE should be in between its performance when compared to uncorrected fluxes and its performance when evaluated against corrected fluxes.

Table 1. Summary of modelled fluxes against the energy balance corrected fluxes, and measured, uncorrected fluxes against the residuals of energy balance from half-hourly to monthly scales.

Temporal scales	Variables x	Variables y	Slope	Intercept (bias)	R^2	RMSE
Half-hourly						
	H_CORR	Modelled H	0.27	7.62	0.47	43.87
	LE_CORR	Modelled LE	0.76	4.64	0.78	33.00
	H_F_MDS	H_re	0.90	12.80	0.69	27.87
	LE_F_MDS	LE_re	0.88	14.60	0.76	27.87
Daily						
	H_CORR	Modelled H	0.56	9.50	0.58	19.27
	LE_CORR	Modelled LE	0.72	5.59	0.74	20.66
	H_F_MDS	H_re	1.11	15.60	0.74	23.65
	LE_F_MDS	LE_re	1.08	15.10	0.82	23.65
Weekly						
	H_CORR	Modelled H	0.58	11.70	0.51	17.67
	LE_CORR	Modelled LE	0.70	4.95	0.78	18.23
	H_F_MDS	H_re	1.15	16.70	0.74	24.08
	LE_F_MDS	LE_re	1.13	15.40	0.84	24.08
Monthly						
	H_CORR	Modelled H	0.62	11.70	0.51	16.20
	LE_CORR	Modelled LE	0.68	4.23	0.81	18.27
	H_F_MDS	H_re	1.23	16.60	0.75	24.70
	LE_F_MDS	LE_re	1.18	15.10	0.86	24.70

Finally, the performance of MaxEnt-ETRHEQ in estimating LE at individual sites throughout the temporal scales are also quite accurate. Figure 2 presents the half-hourly predictions of LE at each site, and shows that despite varying accuracy across different sites, MaxEnt-ETRHEQ demonstrates high precision in predicting half-hourly LE, with R^2 values between 0.74 to 0.89 and RMSE ranging from 20.03 to 53.23 $W \cdot m^{-2}$. However, the predictions of H at various

temporal scales were not satisfactory (Figure S1, Figure S2 and Figure S3). Nevertheless, when the time scale is at the daily, weekly or monthly, both H and LE estimations are improved (Figure 3, Figure S2 and Figure S3). Considering that no site-specific calibration was made, and no T_s or G were used as inputs, the performance of MaxEnt-ETRHEQ at individual sites were excellent.

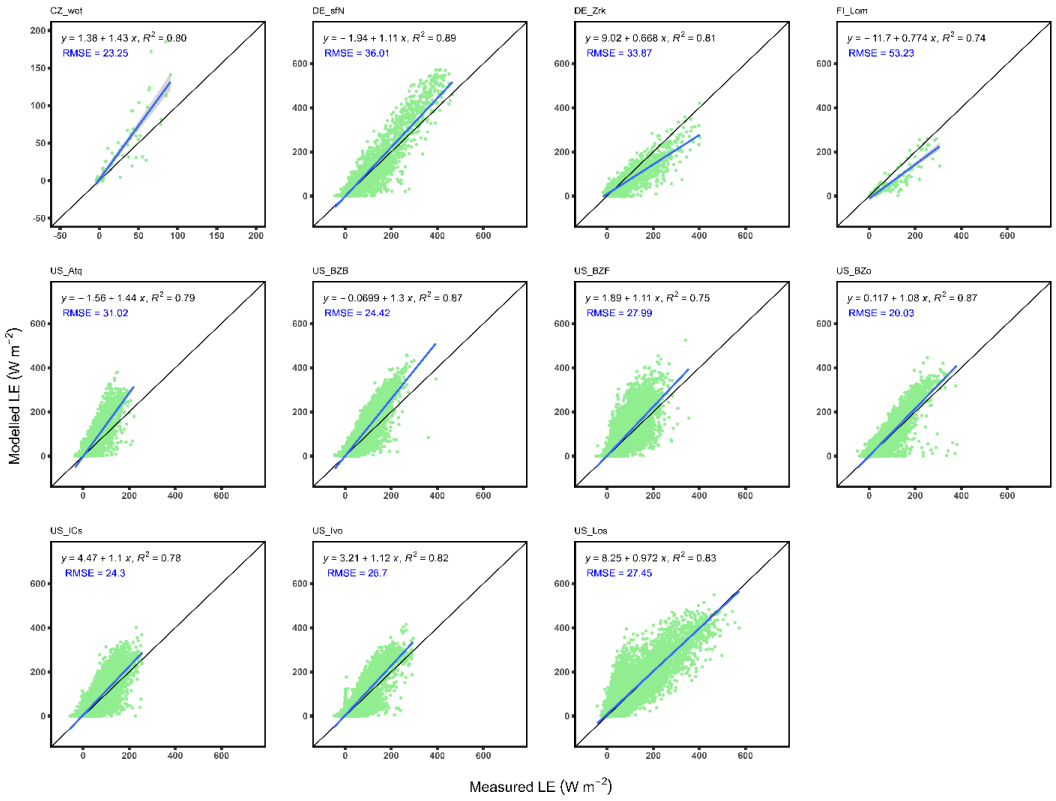

Figure 2. Modelled LE versus measured LE without energy balance closure correction at the half-hourly scale at the study sites. The blue lines represent the fitted linear regressions. Black lines represent 1:1 lines.

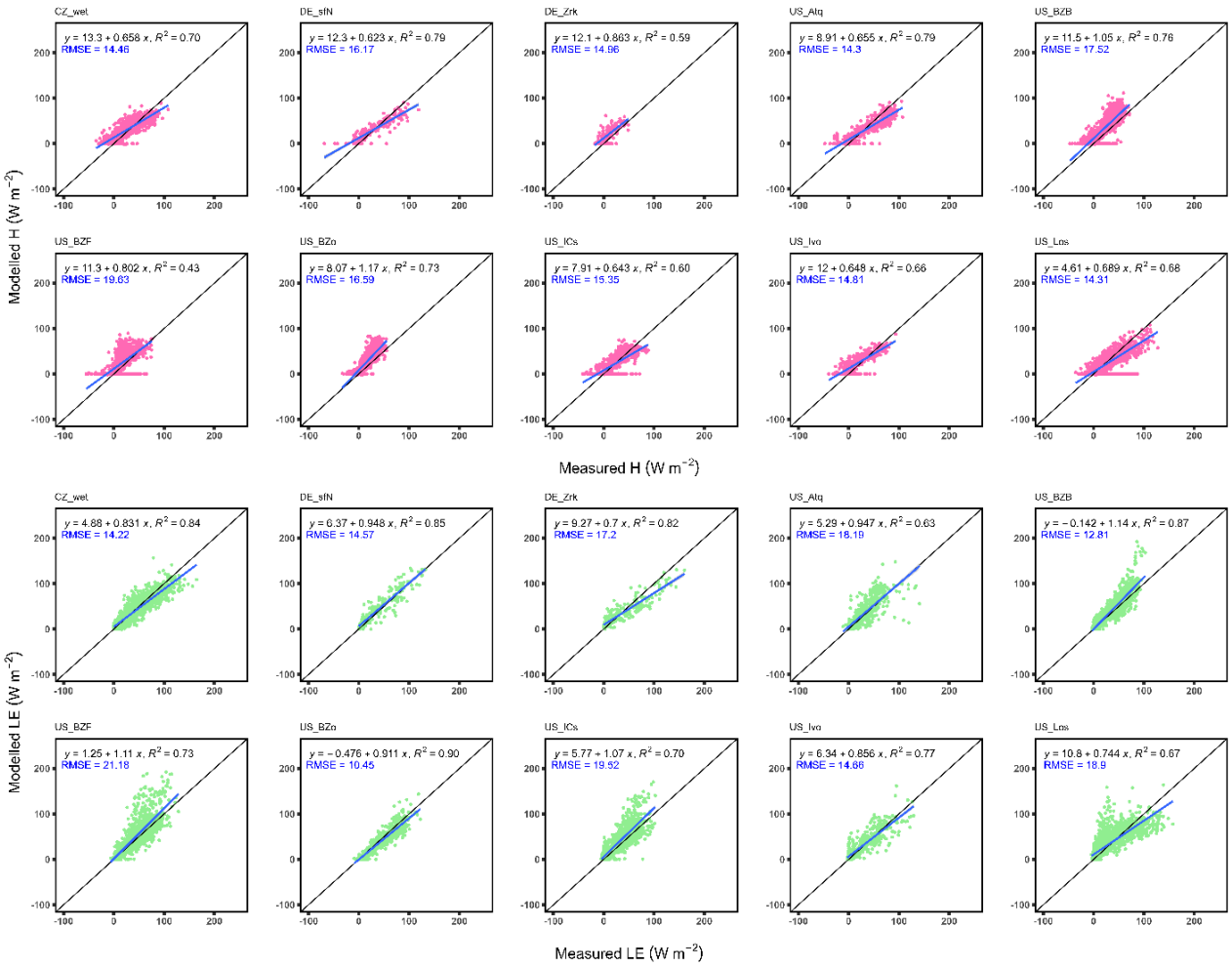

Figure 3. Modelled H and LE versus measured H and LE without energy balance closure correction at the daily scale at the study sites. The blue lines represent the fitted linear regressions, and black lines d1:1 lines.

5. Model advantages and limitations

The main advantage of MaxEnt-ETRHEQ is that it does not require land surface measurements like G and T_s, which outcompetes most evapotranspiration (ET) models. While it could be argued that ET from wetland ecosystems closely approximates potential ET, which can be easily calculated using the Priestley-Taylor or Penman-Monteith equations for saturated water surfaces, the computation of potential ET (PET) still necessitates at least G as input. Additionally,

wetlands may not consistently be in a state of saturation (Streich, 2019), and using these equations could lead to substantial bias.

Moreover, MaxEnt-ETRHEQ is capable of providing estimates of LE at half-hourly intervals, distinguishing it from most equilibrium-based models that require equilibration times that typically extend beyond a daily timeframe, including the SFE model (McColl and Rigden, 2020) and the SFE-MEP model (Kim et al., 2023). The highly accurate half-hourly LE estimates provided by MaxEnt-ETRHEQ mean that the model is capable of precisely capturing the sub-daily fluctuations of ET. Many land surface models have shown considerable inaccuracies in sub-daily LE estimates, typically underestimating LE in the morning and overestimating it in the afternoon, owing to insufficient parameterizations of stomatal conductance and plant hydraulics (Matheny et al., 2014). MaxEnt-ETRHEQ and its underlying mechanism (i.e., the maximum entropy production) may provide new perspectives to enhance the performance of these models.

However, MaxEnt-ETRHEQ is still in its early stages, as further efforts are required to accurately refine the ranges of G, T_s and RH_s. However, that does not mean that these land surface variables ought to be inputs for MaxEnt-ETRHEQ. Rather, identifying appropriate boundary conditions for these variables should suffice. With growing evidence showing the interactions between land surface variables like G, T_s, soil moisture, soil thermal inertia and vegetation properties and near-surface atmospheric conditions (Bennett et al., 2008; Chu et al., 2018; Purdy et al., 2016; Wang and Bras, 1999; Wang and Bou-Zeid, 2012), developing physical models to describe these linkages and determining the limiting cases for G, T_s and RH_s are not far off. Once these boundary conditions are defined properly, MaxEnt-ETRHEQ will be capable of simultaneously estimating not only H, LE, and G, but also T_s and RH_s. Thus, it opens up a promising avenue for future research.

In addition, it may be argued that MaxEnt-ETRHEQ relies on empirical parameters like the parameterization of I_s and g_a. Indeed, most models for estimating surface energy fluxes are largely based on empirical approaches, particularly in calculating parameters such as displacement height, roughness length for momentum and heat transfer, and aerodynamic conductance. Furthermore, when these models are scaled up for application over extensive areas, the reliance on parameters that have been either assumed or previously calibrated becomes inevitable. Therefore, the use of empirical parameterizations in MaxEnt-ETRHEQ should not be viewed as shortcomings. Instead, it underscores the critical need for further research aimed at refining these parameters to enhance the model's accuracy.

6. Conclusion

The goal of this paper is to demonstrate the effectiveness of a newly developed formulation grounded in the principle of maximum Shannon information entropy production theory for estimating surface energy fluxes in wetland ecosystems. The formulation requires neither land surface variables nor site-specific calibration, except for a presumed vegetation height, and it effectively estimates LE from half-hourly to monthly scales in the FLUXNET and AmeriFlux wetland sites. While its estimation on H is less satisfactory due to roughly constrained boundary conditions for G and T_s, the formulation holds promise for concurrently and accurately estimating LE, H, G, T_s and RH_s for various ecosystems if limiting cases of G, Ts and RHs are properly established. Overall, the formulation contributes new insights into developing earth systems models.

Open research

All datasets in this study, as well as the R scripts used for modeling and data visualization, are publicly available. For access to the specific datasets used in this study, please refer to the FLUXNET database (http://www.fluxnet.org) and the AmeriFlux network (http://ameriflux.lbl.gov). For the data analysis, the R programming language version 4.3.0 (R Core Team 2023) was employed. The codes can be accessed on Wang, Y. (2024). R scripts for the submission by Wang and Petrone, "An effective formulation for estimating wetland surface energy fluxes from weather data". Zenodo. https://doi.org/10.5281/zenodo.10602494.

Acknowledgement

The authors wish to express their gratitude to the FLUXNET community and AmeriFlux network for providing access to the invaluable datasets. This work used eddy covariance data acquired and shared by the FLUXNET community, including these networks: AmeriFlux, AfriFlux, AsiaFlux, CarboAfrica, CarboEuropeIP, CarboItaly, CarboMont, ChinaFlux, Fluxnet-Canada, GreenGrass, ICOS, KoFlux, LBA, NECC, OzFlux-TERN, TCOS-Siberia, and USCCC. The FLUXNET eddy covariance data processing and harmonization was carried out by the ICOS Ecosystem Thematic Center, AmeriFlux Management Project and Fluxdata project of FLUXNET, with the support of CDIAC, and the OzFlux, ChinaFlux and AsiaFlux offices. We also acknowledge the following AmeriFlux sites for their data records: US-BZB, US-BZF, US-BZo and US-ICs. In addition, funding for AmeriFlux data resources was provided by the U.S. Department of Energy's Office of Science.

Funding information

We would like to thank the Mountain Water Futures project of the Global Water Futures programme (Canada First Research Excellence Fund), Alberta Innovates – Energy and Environment Solutions (Grant #'s: AIES-2335, 2335 20007947; Rooney, Petrone), and the Canadian Natural Science and Engineering Research Council (NSERC) Discovery (RGPN-04182-2017; Petrone) and CREATE (463960-2015; Petrone) grants programs for the financial support.

References:

Allen, R.G., Pereira, L.S., Raes, D. and Smith, M., 1998. Crop evapotranspiration-Guidelines for computing crop water requirements-FAO Irrigation and drainage paper 56. FAO, Rome, 300(9): D05109.

Arneth, A., Mercado, L., Kattge, J. and Booth, B.B.B., 2012. Future challenges of representing land-processes in studies on land-atmosphere interactions. Biogeosciences, 9(9): 3587-3599.

Aurela, M. et al., 2016. FLUXNET2015 FI-Lom Lompolojankka, FluxNet; Finnish Meteorological Institute.

Bennett, W.B., Wang, J. and Bras, R.L., 2008. Estimation of Global Ground Heat Flux. Journal of Hydrometeorology, 9(4): 744-759.

Chen, S., McColl, K.A., Berg, A. and Huang, Y., 2021. Surface flux equilibrium estimates of evapotranspiration at large spatial scales. Journal of Hydrometeorology, 22(4): 765-779.

Choudhury, B.J., Reginato, R.J. and Idso, S.B., 1986. An analysis of infrared temperature observations over wheat and calculation of latent heat flux. Agricultural and Forest Meteorology, 37(1): 75-88.

Chu, H. et al., 2018. Temporal dynamics of aerodynamic canopy height derived from eddy covariance momentum flux data across North American flux networks. Geophysical research letters, 45(17): 9275-9287.

Desai, A., 2016. FLUXNET2015 US-Los Lost Creek, FluxNet; Univ. of Wisconsin, Madison, WI (United States).

Dewar, R.C., 2005. Maximum entropy production and the fluctuation theorem. Journal of Physics A: Mathematical and General, 38(21): L371.

Dickinson, R.E., Henderson-Sellers, A., Rosenzweig, C. and Sellers, P.J., 1991. Evapotranspiration models with canopy resistance for use in climate models, a review. Agricultural and Forest Meteorology, 54(2): 373-388.

Dušek, J. et al., 2016. FLUXNET2015 CZ-wet Trebon (CZECHWET), FluxNet; Global Change Research Institute CAS.

Duveiller, G., Hooker, J. and Cescatti, A., 2018. The mark of vegetation change on Earth's surface energy balance. Nat Commun, 9(1): 679.

Euskirchen, E., 2021a. AmeriFlux AmeriFlux US-BZB Bonanza Creek Thermokarst Bog, Lawrence Berkeley National Lab.(LBNL), Berkeley, CA (United States ….

Euskirchen, E., 2021b. AmeriFlux AmeriFlux US-BZF Bonanza Creek Rich Fen, Lawrence Berkeley National Lab.(LBNL), Berkeley, CA (United States ….

Euskirchen, E., 2022. AmeriFlux FLUXNET-1F US-BZo Bonanza Creek Old Thermokarst Bog, Lawrence Berkeley National Lab.(LBNL), Berkeley, CA (United States ….

Euskirchen, E., Shaver, G. and Bret-Harte, S., 2016. AmeriFlux AmeriFlux US-ICs Imnavait Creek watershed wet sedge tundra, Lawrence Berkeley National Lab.(LBNL), Berkeley, CA (United States ….

Forzieri, G. et al., 2020. Increased control of vegetation on global terrestrial energy fluxes. Nature Climate Change, 10(4): 356-362.

Good, E.J., Ghent, D.J., Bulgin, C.E. and Remedios, J.J., 2017. A spatiotemporal analysis of the relationship between near-surface air temperature and satellite land surface temperatures using 17 years of data from the ATSR series. Journal of Geophysical Research: Atmospheres, 122(17): 9185-9210.

Green, J.K. et al., 2017. Regionally strong feedbacks between the atmosphere and terrestrial biosphere. Nature Geoscience, 10(6): 410-414.

Huang, S.-Y., Deng, Y. and Wang, J., 2017. Revisiting the global surface energy budgets with maximum-entropy-production model of surface heat fluxes. Climate Dynamics, 49(5): 1531-1545.

Kim, Y., Garcia, M., Black, T.A. and Johnson, M.S., 2023. Assessing the complementary role of Surface Flux Equilibrium (SFE) theory and Maximum Entropy Production (MEP) principle in the estimation of actual evapotranspiration. Journal of Advances in Modeling Earth Systems, 15(7): e2022MS003224.

Kim, Y. et al., 2021. Relative humidity gradients as a key constraint on terrestrial water and energy fluxes. Hydrol. Earth Syst. Sci., 25(9): 5175-5191.

492 Klatt, J., Schmid, H.P., Mauder, M. and Steinbrecher, R., 2016. FLUXNET2015 DE-SfN
493 Schechenfilz Nord, FluxNet; Karlsruhe Institute of Technology, IMK-IFU.

494 Matheny, A.M. et al., 2014. Characterizing the diurnal patterns of errors in the prediction of
495 evapotranspiration by several land-surface models: An NACP analysis. Journal of
496 Geophysical Research: Biogeosciences, 119(7): 1458-1473.

497 Mauder, M. et al., 2018. Evaluation of energy balance closure adjustment methods by
498 independent evapotranspiration estimates from lysimeters and hydrological simulations.
499 Hydrological Processes, 32(1): 39-50.

500 McColl, K.A. and Rigden, A.J., 2020. Emergent Simplicity of Continental Evapotranspiration.
501 Geophysical Research Letters, 47(6): e2020GL087101.

502 McColl, K.A., Salvucci, G.D. and Gentine, P., 2019. Surface Flux Equilibrium Theory Explains
503 an Empirical Estimate of Water-Limited Daily Evapotranspiration. Journal of Advances
504 in Modeling Earth Systems, 11(7): 2036-2049.

505 Merlin, O. et al., 2011. An Analytical Model of Evaporation Efficiency for Unsaturated Soil
506 Surfaces with an Arbitrary Thickness. Journal of Applied Meteorology and Climatology,
507 50(2): 457-471.

508 Merlin, O. et al., 2016. Modeling soil evaporation efficiency in a range of soil and atmospheric
509 conditions using a meta-analysis approach. Water Resources Research, 52(5): 3663-3684.

510 Mildrexler, D.J., Zhao, M. and Running, S.W., 2011. A global comparison between station air
511 temperatures and MODIS land surface temperatures reveals the cooling role of forests.
512 Journal of Geophysical Research: Biogeosciences, 116(G3).

513 Miralles, D.G. et al., 2011. Global land-surface evaporation estimated from satellite-based
514 observations. Hydrol. Earth Syst. Sci., 15(2): 453-469.

515 Mueller, B. and Seneviratne, S.I., 2014. Systematic land climate and evapotranspiration biases in
516 CMIP5 simulations. Geophysical Research Letters, 41(1): 128-134.

517 Pastorello, G. et al., 2020. The FLUXNET2015 dataset and the ONEFlux processing pipeline for
518 eddy covariance data. Scientific Data, 7(1): 225.

519 Priestley, C.H.B. and Taylor, R.J., 1972. On the Assessment of Surface Heat Flux and
520 Evaporation Using Large-Scale Parameters. Monthly Weather Review, 100(2): 81-92.

521 Purdy, A.J., Fisher, J.B., Goulden, M.L. and Famiglietti, J.S., 2016. Ground heat flux: An
522 analytical review of 6 models evaluated at 88 sites and globally. Journal of Geophysical
523 Research: Biogeosciences, 121(12): 3045-3059.

524 Rigden, A.J. and Salvucci, G.D., 2015. Evapotranspiration based on equilibrated relative
525 humidity (ETRHEQ): Evaluation over the continental U.S. Water Resources Research,
526 51(4): 2951-2973.

527 Rigden, A.J. and Salvucci, G.D., 2017. Stomatal response to humidity and CO2 implicated in
528 recent decline in US evaporation. Global Change Biology, 23(3): 1140-1151.

529 Sachs, T., Wille, C., Larmanou, E. and Franz, D., 2016. FLUXNET2015 DE-Zrk Zarnekow,
530 FluxNet; GFZ German Research Centre for Geosciences.

531 Salvucci, G.D. and Gentine, P., 2013. Emergent relation between surface vapor conductance and
532 relative humidity profiles yields evaporation rates from weather data. Proceedings of the
533 National Academy of Sciences, 110(16): 6287-6291.

534 Streich, S.C., 2019. The hydrological function of a mountain valley-bottom peatland under
535 drought conditions, University of Saskatchewan.

536 Wang, J. and Bras, R., 1999. Ground heat flux estimated from surface soil temperature. Journal
537 of hydrology, 216(3-4): 214-226.

538 Wang, J. and Bras, R., 2011. A model of evapotranspiration based on the theory of maximum
539 entropy production. Water Resources Research, 47(3).

540 Wang, J. and Bras, R.L., 2009. A model of surface heat fluxes based on the theory of maximum
541 entropy production. Water Resources Research, 45(11).

542 Wang, J. and Bras, R.L., 2010. An Extremum Solution of the Monin–Obukhov Similarity
543 Equations. Journal of the Atmospheric Sciences, 67(2): 485-499.

544 Wang, K. and Dickinson, R.E., 2012. A review of global terrestrial evapotranspiration:
545 Observation, modeling, climatology, and climatic variability. Reviews of Geophysics,
546 50(2).

547 Wang, Y., 2024. R scripts for the submission by Wang and Petrone, "An effective formulation for
548 estimating wetland surface energy fluxes from weather data". Zenodo.

549 Wang, Y., Petrone, R.M. and Kompanizare, M., 2023. Towards a unified understanding: the
550 linkage of MaxEnt, ETRHEQ, and SFE Models in estimating evapotranspiration.
551 Submitted to Water Resources Research.

552 Wang, Z.-H. and Bou-Zeid, E., 2012. A novel approach for the estimation of soil ground heat
553 flux. Agricultural and Forest Meteorology, 154-155: 214-221.

554 Williams, I.N. and Torn, M.S., 2015. Vegetation controls on surface heat flux partitioning, and
555 land-atmosphere coupling. Geophysical Research Letters, 42(21): 9416-9424.

Wilson, K.B. et al., 2002. Energy partitioning between latent and sensible heat flux during the warm season at FLUXNET sites. Water Resources Research, 38(12): 30-1-30-11.

Yang, Y., Sun, H., Zhu, M., Wang, J. and Zhang, W., 2022. An R package of maximum entropy production model to estimate 41 years of global evapotranspiration. Journal of Hydrology, 614: 128639.

Zona, D. and Oechel, W., 2016a. FLUXNET2015 US-Atq Atqasuk, FluxNet; San Diego State Univ., CA (United States).

Zona, D. and Oechel, W., 2016b. FLUXNET2015 US-Ivo Ivotuk, FluxNet; San Diego State Univ., CA (United States).